HHS Public Access

Author manuscript

ACS Catal. Author manuscript; available in PMC 2019 August 23.

Published in final edited form as:

ACS Catal. 2018 April 6; 8(4): 2789–2795. doi:10.1021/acscatal.7b04308.

Fast and Selective Photoreduction of CO_2 to CO Catalyzed by a Complex of Carbon Monoxide Dehydrogenase, TiO_2, and Ag Nanoclusters

Liyun Zhang[†], **Mehmet Can**[‡], **Stephen W. Ragsdale**[‡], **Fraser A. Armstrong**[*,†]

[†]Inorganic Chemistry Laboratory, Department of Chemistry, University of Oxford, South Parks Road, Oxford OX1 3QR, United Kingdom

[‡]Department of Biological Chemistry, University of Michigan, Ann Arbor, Michigan 48109-0606, United States

Abstract

Selective, visible-light-driven conversion of CO_2 to CO with a turnover frequency of 20 s^{-1} under visible light irradiation at 25 °C is catalyzed by an aqueous colloidal system comprising a pseudoternary complex formed among carbon monoxide dehydrogenase (CODH), silver nanoclusters stabilized by polymethacrylic acid (AgNCs-PMAA), and TiO_2 nanoparticles. The photocatalytic assembly, which is stable over several hours and for at least 250000 turnovers of the enzyme's active site, was investigated by separate electrochemical (dark) and fluorescence measurements to establish specific connectivities among the components. The data show (a) that a coating of AgNCs-PMAA on TiO_2 greatly enhances its ability as an electrode for CODH- based electrocatalysis of CO_2 reduction and (b) that the individual Ag nanoclusters interact directly and dynamically with the enzyme surface, most likely at exposed cysteine thiols. The results lead to a model for photocatalysis in which the AgNCs act as photosensitizers, CODH captures the excited electrons for catalysis, and TiO_2 mediates hole transfer from the AgNC valence band to sacrificial electron donors. The results greatly increase the benchmark for reversible CO_2 reduction under ambient conditions and demonstrate that, with such efficient catalysts, the limiting factor is the supply of photogenerated electrons.

Graphic abstract

[*]Corresponding Author fraser.armstrong@chem.ox.ac.uk.

Author Contributions

L.Z. designed, carried out and analyzed all experiments. L.Z. and F.A.A. interpreted the results and wrote the manuscript. M.C. and S.W.R. prepared the enzyme and revised the manuscript.

Notes

The authors declare no competing financial interest.

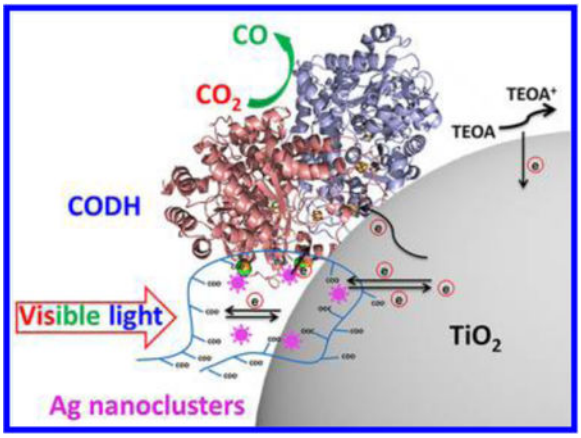

Keywords

carbon monoxide dehydrogenase; silver nanoclusters; artificial photosynthesis; CO_2 photoreduction; photocatalytic enzyme assembly

INTRODUCTION

There is significant economic and scientific interest in converting intermittent solar energy into storable fuels (artificial photosynthesis, AP) and intense efforts are underway to establish ways to produce H_2 from water or reduced carbon compounds from CO_2, in all cases using catalysts based on abundant elements.[1–3] An inspirational approach to photo-H_2 production has been to exploit the extremely high catalytic activity of hydrogenases by attaching them directly to light- harvesting systems.[4–6] Direct reduction of a concentrated source of CO_2 (as present in flue gas) is far more challenging than H_2 production,[7–13] but once again, insight has been derived from metalloenzymes such as carbon monoxide dehydrogenase (CODHs: Ni and Fe)[14] or formate dehydrogenase (FRDs: Mo or W), each of which is highly active in catalyzing two-electron reduction of CO_2 with extreme selectivity, avoiding the thermodynamically easier H_2 evolution.[15–18] Importantly, the activities of these enzymes are so high[19] that the performance of the integrated photocatalytic systems in which they are incorporated is limited not by catalysis but by photophysical restrictions and charge-transport connections. An earlier dilemma was that, despite the high activity and efficiency expected for CODH on the basis of steady-state rates and experiments using protein film electrochemistry (PFE),[20] the photocatalytic per-enzyme-molecule turnover frequency (TOF) was orders of magnitude lower than expected (the initial TOF being just 0.18 s^{-1}).[18] With such an active enzyme, it appeared that the shortcoming lay in low electron availability, as a result of either short excited-state lifetime and/or poor electronic coupling to the enzyme.

Here, we describe the profound effect of silver nanoclusters (AgNCs) on the CO_2 photoreduction activity of CODH (specifically CODH I from *Carboxydothermus hydrogenofor mans*) upon attachment to TiO_2 nanoparticles. Metal nano clusters have special optoelectronic properties due to quantum confinement and behave as molecular redox species: they are under investigation for analytical and energy-related applications, a

particularly relevant one being their use as sensitizers for TiO_2 solar cells.[21] By templating in protective hosts such as polymethacrylic acid (PMAA), AgNCs containing <10 Ag atoms can be stabilized in water.[22,23] The luminescent nanoclusters rapidly reduce methyl viologen upon illumination with visible light.[24] Further, their emission properties are sensitive to interactions with specific ligands such as thiolates,[25] which are often exposed on the surface of proteins. Considering that free carboxylates on PMAA are, in turn, suited for binding to the surface of TiO_2,[26,27] it was reasoned that PMAA-capped AgNCs (AgNCs-PMAA) should form stable connections between CODH and the surface of TiO_2, thereby creating a soft assembly that simultaneously harvests visible light and directs electron and hole transfers to support rapid and efficient CO_2 photoreduction.

EXPERIMENTAL SECTION

Preparation of Silver Nanoclusters (AgNCs).

Silver nanoclusters (AgNCs) were synthesized according to a previously published procedure.[23] A freshly prepared aqueous solution of silver nitrate (0.1 M, 10 mL, Sigma-Aldrich, 99+%) was mixed with an equal volume of PMAA solution (5 mg/mL, adjusted with nitric acid to pH 3.0) at room temperature. After mixing, the colorless solution was purged by N_2 bubbling for 15 min to remove O_2 before exposing to laboratory sunlight. With increasing irradiation time the solution gradually changed from colorless to light pink and then to magenta. The solution was then mixed with tetrahydrofuran (17–30% w/w), and the deep magenta clusters that aggregated upon shaking were removed by centrifugation (3600 rpm, 15 min) and redissolved in water. The concentration of AgNCs was measured by inductively coupled plasma mass spectrometry (ICP-MS, Thermo Element 2). Matrix-assisted laser desorption time-of-flight mass spectra (MALDI-ToF-MS) were recorded on a Bruker Reflex III operated in reflectron mode using a N_2 laser (337 nm) and an accelerating voltage of 20 kV. The sample was prepared by drop-coating the solution onto the target.

Electrochemistry Experiments.

The working electrode consisting of TiO_2 deposited on indium tin oxide (ITO) (see the Supporting Information) was used in a single-compartment electrochemical cell with a Pt (wire) counter electrode, with a saturated calomel reference electrode held in a separate side arm and linked by a Luggin capillary. All potentials are quoted vs the standard hydrogen electrode (SHE) using the conversion relationship $E_{SHE} = E_{SCE} + 241$ mV at 25 °C. The electrolyte consisted of 0.1 M NaCl and 0.2 M MES at pH 6.0, and all solutions were prepared using purified water (Milli-Q, 18 MΩ cm). Electrochemical measurements were carried out with an Autolab potentiostat (PGSTAT30) controlled by Nova software (EcoChemie). Precise gas mixtures (BOC gases) were created using mass flow controllers (Sierra Instruments), and the electrochemical cell was constantly purged with the gas mixture throughout the experiments.

Quantitative Analysis of CO Formed in Photocatalytic Experiments.

An Agilent 7890A series gas chromatograph (GC) with electronic pneumatic control optimized for trace gas analysis was used to monitor CO production at regular intervals. Headspace gas samples (20 μL) were injected into the GC in pulsed splitless mode using a

gastight Hamilton syringe. A 1.5 mm diameter split/splitless liner, a Restek ShinCarbon ST micropacked column, a micro thermal conductivity detector, and high-purity He carrier gas with a constant pressure of 25 psi were used. The column oven was heated from 40 to 200 °C at a rate of 10 °C min^{-1} during measurements.

RESULTS

Photocatalysis.

Figure 1 shows experiments in which an aqueous suspension of CODH/AgNCs-PMAA/TiO_2 sealed under a CO_2 atmosphere was illuminated with visible light. Details for the preparation of AgNCs-PMAA and AgNCs- PMAA/TiO_2 nanomaterials are given in Figures S1–S3 in the Supporting Information. All suspensions were prepared in a glovebox under a N_2 atmosphere before they were taken out for measurements. Briefly, a suspension of AgNCs-PMAA/TiO_2 (5 mg) formed from 3.05 mg of TiO_2 (Evonik Aeroxide P25, 21 nm diameter) and 1.95 mg of AgNCs templated in PMAA (resulting in a final Ag/Ti atomic ratio of 0.27 as determined by ICP-MS) was formed by sonicating the two components in a 5 mL aqueous solution of 0.1 M triethanolamine (TEOA), 0.1 M NaCl, and 25 mM EDTA, adjusted to pH 6.0, all contained in a Pyrex pressure vessel (total volume 22.5 mL). Then CODH (50 μL of 10 μM solution, see the Supporting Information) was added and the suspension was stirred gently for 3 min to allow adsorption of the enzyme, before the vessel was sealed tightly with a rubber septum and the headspace purged with CO_2. The stirred suspension was irradiated with visible light using a 300 W arc lamp (Newport 67005) fitted with a 420 nm filter and held 5 cm from the vessel. The temperature was controlled by immersing the vessel in a water bath. Production of CO was monitored at regular intervals by removing small volumes (20 μL) of headspace gas for gas chromatography (GC) analysis. The amount of CO was quantified against calibration plots obtained with known amounts of CO (Figure S4). Turnover frequencies were obtained by dividing the quantity of CO formed in a given time by the total amount of CODH used.

The results obtained without one of the components present, CODH, TiO_2 or AgNCs-PMAA, are included in Figure 1: the data suggest the requirement for a quasi-ternary complex containing all three components, although not necessarily in a stoichiometric manner (hence “quasi”). The initial turnover frequency (TOF) of 20 s^{-1} observed at 25 °C increases to 37 s^{-1} at 50 °C. At 25 °C the rate of CO production is steady during the first 1 h of irradiation before decreasing gradually to 14 s^{-1} over the next 3 h. Although the underlying stability is one factor, much of this decrease could be attributed to product inhibition by CO because the rate increased substantially each time the headspace was refreshed (Figure 1b). Taking cycle 1 as an example, the CO concentration reaches 6.7% in the headspace before flushing out: assuming a value of 1 mM for Henry’s constant, the corresponding CO concentration in the solution would be 67 μM, a value that exceeds the inhibition constant (46 μM) measured electrochemically under comparable conditions at −560 mV vs SHE.[28] In no case was any H_2 detected by GC: this important result is consistent with previous results[29] showing that CODHs are highly selective Table 1. Visible-Light-Driven CO_2 Reduction by CODH/ AgNCs-PMAA/TiO_2 Assemblies under Different Conditions catalysts for CO_2 reduction even though water reduction is favored

thermodynamically. An interesting and obvious outcome of the experiments shown in Figure 1b is that, after 6 h, each CODH molecule has turned over about 250000 times. Results obtained under a wide range of conditions are shown in Table 1. The rate of CO production varies by less than a factor of 2 among different electron donors (TEOA, EDTA, and MES). No significant changes in CO yield after 30 min irradiation were observed for TEOA concentrations between 0.05 and 0.25 M (Figure S5). Using the filtered light intensity and illuminated facial area of the reaction vessel, we estimated that the quantum yield would be approximately 1.5% on the basis of a wavelength of 500 nm.

The discovery that a quasi-ternary complex formulated as CODH/AgNCs-PMAA/TiO_2 photoreduces CO_2 far more quickly than any binary combination was followed up with studies designed to examine different aspects of the interaction. An estimation of the composition of AgNCs-PMAA (the “soft” and least well-de fined component) was carried out, on the basis of an average molecular weight of 5000 for PMAA. Taking, as a reference point, Ag_5 to be the dominant nanocluster (Figure S1), the analytical mass ratio 1/0.53 determined by ICP-MS yielded 5 Ag_5 per polymer molecule. Each PMAA has approximately 60 monomer units; therefore, numerous carboxylates should remain free to bind to the TiO_2 surface.[26]

Electrocatalysis.

To investigate how AgNCs influence the “dark” electrocatalytic CO_2/CO interconversion by CODH at a TiO_2 surface, experiments were carried out in which an electrode consisting of TiO_2 deposited on indium tin oxide (ITO) was modified with various combinations of AgNCs- PMAA, PMAA alone, and CODH. The results are shown in Figure 2.

An unmodified TiO_2 electrode displays a signature “trumpet shaped” voltammogram that may be interpreted, chemically, in terms of the electronic conductivity increasing at the most negative potential as Ti(IV) centers are converted to Ti(III).[16] Comparisons between catalytic cyclic voltammograms (CVs) of CODH adsorbed at a TiO_2 electrode (Figure 2a) and at an AgNCs-PMAA/TiO_2 electrode (Figure 2b) reveal that CO_2 reduction activity is greatly enhanced by the presence of AgNCs-PMAA, which causes the current to increase at a lower overpotential. A small current due to reoxidation of CO becomes detectable, and there is also a change in the “background” control voltammogram (no CODH) when AgNCs-PMAA is present. Proof that the catalytic current stems from enzymatic activity was obtained by injecting an aliquot of concentrated KOCN solution into the cell (to a final concentration of 60 mM). Cyanate (NCO^-), which is isoelectronic with CO_2, targets the C_{red2} state of the enzyme and blocks CO_2 reduction.[28] Figure 2c depicts the selective inhibition of CO_2 reduction on a CODH/AgNCs-PMAA/TiO_2 electrode after adding KOCN. Comparison of the background traces in Figure 2a,b shows that modification of the TiO_2 electrode with AgNCs-PMAA leads to a new reduction peak at −0.56 V (vs SHE), similar to that attributed to trap surface states of TiO_2 introduced particularly by binding of oxygen atom donor ligands.[30,31] Figure 2d shows that PMAA alone (without AgNCs) also gives rise to a change in the TiO_2 background, introducing a small reduction peak similar to that observed with AgNCs-PMAA but shifted to more positive potential. Importantly, no

catalytic current is observed when CODH is introduced, indicating that PMAA alone blocks the electrode with regard to electron transfer, enzyme binding, or both.

Experiments to determine the stability and temperature dependence of the catalytic current were carried out: *C. hydrogenoformans* is a thermophile, and CODH should be inherently stable at ambient temperatures.[32] The temperature dependence of CO_2 reduction activity at a CODH/AgNCs- PMAA/TiO_2 electrode over the range 25–50 °C is shown in Figure S6, while Figures S7 and S8 show the stabilities determined by cyclic voltammetry and chronoamperometry, respectively. Cyclic voltammograms obtained under 100% CO_2 showed only a small decrease in current over 24 h, and chronoamperometry at −0.66 V vs SHE revealed even a small improvement with time. Both results reinforce the observations of the photocatalytic time courses for CO production with colloidal CODH/AgNCs-PMAA/TiO_2 and highlight the stark contrast with earlier results obtained with a RuP—TiO_2 system.[18,33] The fact that increasing the temperature from 25 to 50 °C yields only a modest (less than 2-fold) increase in rate suggests that CO_2 reduction at the active site of the enzyme (a [Ni4Fe-4S] cofactor known as the "C-cluster"[14,20]) is still not a limiting factor.

Fluorescence.

The speci fic interaction between PMAA-stabilized AgNCs and CODH was studied by performing a photoluminescence (PL) titration along with nanosecond luminescence kinetics. As shown in Figure 3a, the emission intensity first decreases and then increases as CODH is added to a solution containing AgNCs-PMAA. The point at which emission is minimal should correspond to optimal formation of a CODH/AgNCs-PMAA complex, which in this case (Ag atom concentration 20 μM) occurs when the CODH concentration is 0.54 μM. However, due to the coexistence of different structures and compositions in AgNCs-PMAA solution (Figure S1), the binding stoichiometry and a meaningful dissociation constant (K_d) between AgNCs-PMAA and CODH cannot be determined.

The mechanism of photoemission by metal nanoclusters is controversial,[34–37] and independent studies have shown that the natures of the nanocluster core and anchoring ligands are both important. The quenching of emission that is observed as aliquots of CODH are added to AgNCs-PMAA resembles the quenching that is observed specifically in the presence of cysteine.[25] The subsequent increase (Figure 3a and Figure S9 peak I′ at 544 nm) and appearance of a new blue-shifted emission peak (Figure S9 peak II′ at 522 nm) at higher CODH concentration suggests that further reactions occur beyond the binding of cysteine thiolate to Ag (see Figure S10).

Time-correlated single photon counting (TCSPC) provided further information about the charge-transfer dynamics underlying the AgNCs fluorescence quenching (Figure 3b and Table S1). The short lifetime for Ag nanoclusters is typical for metal core sp—d hole recombination (fluorescence originating from the recombination of electrons in the s−p band with holes in the d band).[38] The longer emission lifetime observed in the presence of CODH suggests surface-state sensitivity:[39] specifically, in this case, an interaction between the metal core and the thiolate-S.[38,40]

DISCUSSION

Although the structure of CODH I has not been solved, some idea of the availability of surface cysteines is obtained from the structure of CODH II (1SU7)[41] and the CODH (CODH *Rr*) from *Rhodospirillum rubrum* (1JQK).[42] A model for CODH I based on CODH-*Rr* using the SWISS-MODEL web program was simulated (Figure S11), and four possible surface cysteines were predicted for each half of the enzyme, these being cys162, cys271, cys346, and cys401. Of these possibilities, one cysteine (346) is conserved and surface exposed in the structure of CODH II and CODH *Rr*. Although the surface-exposed cysteine appears to be too remote to allow a direct electron transfer into the enzyme, it is likely that such a residue acts as an anchor point by which one Ag nanocluster is bound, the overall effect being to bring CODH, TiO_2, and other PMAA- stabilized AgNCs into dynamic close contact.

Attempting to explain the interactions within a pseudoternary assembly in which the “soft” AgNCs-PMAA is a crucial component required an empirical approach. The connectivities among CODH, AgNCs, PMAA, and TiO_2, in terms of all the experiments carried out, are therefore presented in Scheme 1. Whether measured by electrocatalysis (E) or photocatalysis (P), the ternary system outperforms the binary CODH/TiO_2 system by about 2 orders of magnitude and the activity is much longer lived. The fact that the CODH/PMAA/TiO_2 system (lacking AgNCs) is inactive electrochemically shows that any surface trap states that are introduced play no role the PMAA acting instead to block electron transfer.

Referring to Table 1, rates of photocatalysis scale with the amount of enzyme in the system, and notably, for each given quantity of CODH, the rate of CO production is independent of the amount of AgNCs-PMAA/TiO_2.These results show that the Ag nanoclusters are not acting directly as reduction catalysts.[43–45] Instead, since CO_2 reduction is driven by visible light and not UV (as would be required for bandgap excitation of TiO_2), the Ag nanoclusters must be operating as photosensitizers. The report that photoexcited AgNCs are highly proficient in reducing methylviologen is consistent with a calculation by Chen et al. indicating that the LUMO of a AgNC is 0.26 eV higher in energy than the conduction band of TiO_2 (itself capable of reducing CO_2).[43] Although this energy gap means that electrons could pass from photoexcited AgNCs to TiO_2, and then to enzyme, the electrochemical evidence discussed in more detail below suggests that electrons could instead transfer directly from photoexcited AgNCs to CODH and thence rapidly reduce CO_2, the catalytic efficiency of the enzyme providing such an effective trap.

From the electrocatalysis experiments, AgNCs-PMAA adsorbed on TiO_2 promotes CO_2 reduction by CODH at a higher potential (lower overpotential) in comparison to TiO_2 alone, whereas PMAA alone, which also produces a surface- state redox transition, completely blocks electrocatalysis. Therefore, the AgNCs contained in PMAA are acting as electron mediators to the coadsorbed enzyme. The AgNCs embedded in PMAA must therefore be capable of rapid motion within the polymer, fast intercluster electron transfer, or both. The specific binding of CODH to Ag nanoclusters that is observed by fluorescence (F) helps to account for the photocatalytic activity that is displayed (at a much lower level) by the binary system CODH/AgNCs-PMAA. On the basis of the selective interaction with cysteine

reported by others,[25] we expect that one or two surface-exposed cysteines are the primary targets, the interaction being dynamic and short-lived in order to account for the fact that the fluorescence is completely quenched during the titration. The surface- exposed cysteine thiolates on CODH are too remote to allow direct electron transfer to the active site from a transiently interacting AgNC, but a dynamic arrangement and/or fast electron transfer between AgNCs within the same PMAA particle would allow use of the surface-exposed D cluster.[46]

The increased catalytic activity observed for the quasi-ternary assembly that includes TiO_2 in comparison to CODH/AgNCs- PMAA alone suggests that the TiO_2 nanoparticle is more than just a supporting scaffold. An estimate indicates that on average at least two CODH molecules may be loaded onto a single AgNCs-PMAA/TiO_2 nanoparticle (calculation given in the Supporting Information). On the basis of a proposal by Wang and co-workers,[43] the most likely mechanistic role for TiO_2 is to mediate hole transfer from the AgNC valence band to sacrificial electron donors reacting at its surface.

CONCLUSION

In summary, a stable, quasi-ternary complex of CODH coadsorbed on TiO_2 nanoparticles with PMAA-stabilized Ag nanoclusters displays specific reduction of CO_2 to CO under visible light, at a per-CODH rate that is 2 orders of magnitude higher and much more stable than that reported earlier when a photosensitizing RuP complex was used.[18] The findings raise interesting questions about the overall mechanism, important details of which remain to be clarified. The results help to emphasize the value of using enzymes in investigations of colloidal photocatalysts: their superb abilities as fast, efficient, and selective electrocatalysts focuses attention instead on the limitations affecting the light-harvesting and charge-transfer components and the directions needed for major improvements, including capitalizing on what is already known about the interaction of CODH with CO_2 and CO.[14]

Supplementary Material

Refer to Web version on PubMed Central for supplementary material.

ACKNOWLEDGMENTS

L. Z. thanks the Royal Society and Newton fund for a Newton international fellow award (DHR00490). F.A.A. is a Royal Society−Wolfson Research Merit Award holder: research in his laboratory has been supported by several grants from the UK Biotechnology and Biological Sciences Research Council (BBSRC) particularly BB/M005720/1. We thank Professor Stephen Faulkner for allowing us to use his fluorescence spectrometer.

REFERENCES

(1). Gust D; Moore TA; Moore AL Solar Fuels via Artificial Photosynthesis. Acc. Chem. Res 2009, 42, 1890–1898. [PubMed: 19902921]

(2). Kim D; Sakimoto KK; Hong DC; Yang PD Artificial Photosynthesis for Sustainable Fuel and Chemical Production. Angew. Chem., Int. Ed 2015, 54, 3259–3266.

(3). Lewis NS; Nocera DG Powering the Planet: Chemical Challenges in Solar Energy Utilization. Proc. Natl. Acad. Sci. U. S. A 2006, 103, 15729–15735. [PubMed: 17043226]

(4). Bachmeier A; Armstrong F Solar-driven Proton and Carbon Dioxide Reduction to Fuels Lessons from Metalloenzymes. Curr. Opin. Chem. Biol 2015, 25, 141–151. [PubMed: 25621455]

(5). Brown KA; Wilker MB; Boehm M; Dukovic G; King PW Characterization of Photochemical Processes for H_2 Production by CdS Nanorod−[FeFe] Hydrogenase Complexes. J. Am. Chem. Soc 2012, 134, 5627–5636. [PubMed: 22352762]

(6). Woolerton TW; Sheard S; Chaudhary YS; Armstrong FA Enzymes and Bio-inspired Electrocatalysts in Solar Fuel Devices. Energy Environ. Sci 2012, 5, 7470–7490.

(7). Wu Y; Rudshteyn B; Zhanaidarova A; Froehlich JD; Ding W; Kubiak CP; Batista VS Electrode-Ligand Interactions Dramatically Enhance CO_2 Conversion to CO by the [Ni(cyclam)]- $(PF_6)_2$ Catalyst. ACS Catal 2017, 7, 5282–5288.

(8). Urbain F; Tang P; Carretero NM; Andreu T; Gerling LG; Voz C; Arbiol J; Morante JR A Prototype Reactor for Highly Selective Solar-driven CO_2 Reduction to Synthesis Gas Using Nanosized Earth-abundant Catalysts and Silicon Photovoltaics. Energy Environ. Sci 2017, 10, 2256–2266.

(9). Schreier M; Heŕoguel F; Steier L; Ahmad S; Luterbacher JS; Mayer MT; Luo J; Graẗzel M Solar Conversion of CO_2 to CO Using Earth-abundant Electrocatalysts Prepared by Atomic Layer Modification of CuO. Nat. Energy 2017, 2, 17087.

(10). Liu X; Xiao J; Peng H; Hong X; Chan K; Nørskov JK Understanding Trends in Electrochemical Carbon Dioxide Reduction Rates. Nat. Commun 2017, 8, 15438. [PubMed: 28530224]

(11). Jovanov ZP; Hansen HA; Varela AS; Malacrida P; Peterson AA; Nørskov JK; Stephens IEL; Chorkendorff I Opportunities and Challenges in the Electrocatalysis of CO_2 and CO Reduction Using Bifunctional Surfaces: A Theoretical and Experimental Study of Au−Cd Alloys. J. Catal 2016, 343, 215–231.

(12). Wang WH; Himeda Y; Muckerman JT; Manbeck GF; Fujita E CO_2 Hydrogenation to Formate and Methanol as an Alternative to Photo- and Electrochemical CO_2 Reduction. Chem. Rev 2015, 115, 12936–12973. [PubMed: 26335851]

(13). Kortlever R; Balemans C; Kwon Y; Koper MTM Electrochemical CO_2 Reduction to Formic Acid on a Pd-based Formic Acid Oxidation Catalyst. Catal. Today 2015, 244, 58–62.

(14). Can M; Armstrong FA; Ragsdale SW Structure, Function, and Mechanism of the Nickel Metalloenzymes, CO Dehydrogenase, and Acetyl-CoA Synthase. Chem. Rev 2014, 114, 4149–4174. [PubMed: 24521136]

(15). Bachmeier A; Hall S; Ragsdale SW; Armstrong FA Selective Visible-Light-Driven CO_2 Reduction on a p-Type Dye- Sensitized NiO Photocathode. J. Am. Chem. Soc 2014, 136, 13518–13521. [PubMed: 25237714]

(16). Bachmeier A; Wang VCC; Woolerton TW; Bell S; Fontecilla-Camps JC; Can M; Ragsdale SW; Chaudhary YS; Armstrong FA How Light-Harvesting Semiconductors Can Alter the Bias of Reversible Electrocatalysts in Favor of H_2 Production and CO_2 Reduction. J. Am. Chem. Soc 2013, 135, 15026–15032. [PubMed: 24070184]

(17). Chaudhary YS; Woolerton TW; Allen CS; Warner JH; Pierce E; Ragsdale SW; Armstrong FA Visible Light-driven CO_2 Reduction by Enzyme Coupled CdS Nanocrystals. Chem. Commun 2012, 48, 58–60.

(18). Woolerton TW; Sheard S; Pierce E; Ragsdale SW; Armstrong FA CO_2 Photoreduction at Enzyme-modified Metal Oxide Nanoparticles. Energy Environ. Sci 2011, 4, 2393–2399.

(19). Armstrong FA; Hirst J Reversibility and Efficiency in Electrocatalytic Energy Conversion and Lessons from Enzymes. Proc. Natl. Acad. Sci. U. S. A 2011, 108, 14049–14054. [PubMed: 21844379]

(20). Parkin A; Seravalli J; Vincent KA; Ragsdale SW; Armstrong FA Rapid and Efficient Electrocatalytic CO_2/CO Interconversions by Carboxydothermus hydrogenoformans CO Dehydrogenase I on an Electrode. J. Am. Chem. Soc 2007, 129, 10328–10329. [PubMed: 17672466]

(21). Chen Y-S; Choi H; Kamat PV Metal-Cluster-Sensitized Solar Cells. A New Class of Thiolated Gold Sensitizers Delivering Efficiency Greater Than 2%. J. Am. Chem. Soc 2013, 135, 8822–8825. [PubMed: 23718130]

(22). Xu H; Suslick KS Sonochemical Synthesis of Highly Fluorescent Ag Nanoclusters. ACS Nano 2010, 4, 3209–3214. [PubMed: 20507161]

(23). Diez I; Pusa M; Kulmala S; Jiang H; Walther A; Goldmann AS; Muller AHE; Ikkala O; Ras RHA Color Tunability and Electrochemiluminescence of Silver Nanoclusters. Angew. Chem., Int. Ed 2009, 48, 2122–2125.

(24). Chen W-T; Hsu Y-J; Kamat PV Realizing Visible Photoactivity of Metal Nanoparticles: Excited-State Behavior and Electron-Transfer Properties of Silver (Ag_8) Clusters. J. Phys. Chem. Lett 2012, 3, 2493–2499. [PubMed: 26292139]

(25). Shang L; Dong S Sensitive Detection of Cysteine based on Fluorescent Silver Clusters. Biosens. Bioelectron 2009, 24, 1569–1573. [PubMed: 18823770]

(26). Brennan BJ; Portoles MJL; Liddell PA; Moore TA; Moore AL; Gust D Comparison of Silatrane, Phosphonic Acid, and Carboxylic acid Functional Groups for Attachment of Porphyrin Sensitizers to TiO_2 in Photoelectrochemical Cells. Phys. Chem. Chem. Phys 2013, 15, 16605–16614. [PubMed: 23959453]

(27). Brown DG; Schauer PA; Borau-Garcia J; Fancy BR; Berlinguette CP Stabilization of Ruthenium Sensitizers to TiO_2 Surfaces through Cooperative Anchoring Groups. J. Am. Chem. Soc 2013, 135, 1692–1695. [PubMed: 23343106]

(28). Wang VC; Can M; Pierce E; Ragsdale SW; Armstrong FA A Unified Electrocatalytic Description of the Action of Inhibitors of Nickel Carbon Monoxide Dehydrogenase. J. Am. Chem. Soc 2013, 135, 2198–206. [PubMed: 23368960]

(29). Wang VC; Islam ST; Can M; Ragsdale SW; Armstrong FA Investigations by Protein Film Electrochemistry of Alternative Reactions of Nickel-Containing Carbon Monoxide Dehydrogenase. J. Phys. Chem. B 2015, 119, 13690–13697. [PubMed: 26176986]

(30). Jankulovska M; Berger T; Wong SS; Gómez R; Lana-Villarreal T Trap States in TiO_2 Films Made of Nanowires, Nanotubes or Nanoparticles: An Electrochemical Study. ChemPhy-sChem 2012, 13, 3008–3017.

(31). De la Garza L; Saponjic ZV; Dimitrijevic NM; Thurnauer MC; Rajh T Surface States of Titanium Dioxide Nanoparticles Modified with Enediol Ligands. J. Phys. Chem. B 2006, 110, 680–686. [PubMed: 16471588]

(32). Svetlitchnyi V; Peschel C; Acker G; Meyer O Two Membrane-Associated NiFeS-Carbon Monoxide Dehydrogenases from the Anaerobic Carbon-Monoxide-Utilizing Eubacterium Carbox- ydothermus hydrogenoformans. J. Bacteriol 2001, 183, 5134–5144. [PubMed: 11489867]

(33). Woolerton TW; Sheard S; Reisner E; Pierce E; Ragsdale SW; Armstrong FA Efficient and Clean Photoreduction of CO_2 to CO by Enzyme-Modified TiO_2 Nanoparticles Using Visible Light. J. Am. Chem. Soc 2010, 132, 2132–2133. [PubMed: 20121138]

(34). Luo Z; Yuan X; Yu Y; Zhang Q; Leong DT; Lee JY; Xie J From Aggregation-Induced Emission of Au(I)−Thiolate Complexes to Ultrabright Au(0)@Au(I)−Thiolate Core−Shell Nano- clusters. J. Am. Chem. Soc 2012, 134, 16662–16670. [PubMed: 22998450]

(35). Wu Z; Jin R On the Ligand's Role in the Fluorescence of Gold Nanoclusters. Nano Lett 2010, 10, 2568–2573. [PubMed: 20550101]

(36). Chen Y; Yang T; Pan H; Yuan Y; Chen L; Liu M; Zhang K; Zhang S; Wu P; Xu J Photoemission Mechanism of Water- Soluble Silver Nanoclusters: Ligand-to-Metal−Metal Charge Transfer vs Strong Coupling between Surface Plasmon and Emitters. J. Am. Chem. Soc 2014, 136, 1686–1689. [PubMed: 24437963]

(37). Diez I; Ras RHA; Kanyuk MI; Demchenko AP On Heterogeneity in Fluorescent Few-atom Silver Nanoclusters. Phys. Chem. Chem. Phys 2013, 15, 979–985. [PubMed: 23212676]

(38). Zhu M; Aikens CM; Hollander FJ; Schatz GC; Jin R Correlating the Crystal Structure of A Thiol-Protected Au_{25} Cluster and Optical Properties. J. Am. Chem. Soc 2008, 130, 5883–5885. [PubMed: 18407639]

(39). Yau SH; Abeyasinghe N; Orr M; Upton L; Varnavski O; Werner JH; Yeh H-C; Sharma J; Shreve AP; Martinez JS; Goodson Iii T Bright Two-photon Emission and Ultra-fast Relaxation Dynamics in a DNA-templated Nanocluster Investigated by Ultra-fast Spectroscopy. Nanoscale 2012, 4, 4247–4254. [PubMed: 22692295]

(40). Miller SA; Womick JM; Parker JF; Murray RW; Moran AM Femtosecond Relaxation Dynamics of $Au_{25}L18^-$ Monolayer-Protected Clusters. J. Phys. Chem. C 2009, 113, 9440–9444.

(41). Dobbek H; Svetlitchnyi V; Liss J; Meyer O Carbon Monoxide Induced Decomposition of the Active Site [Ni−4Fe−5S] Cluster of CO Dehydrogenase. J. Am. Chem. Soc 2004, 126, 5382–5387. [PubMed: 15113209]

(42). Drennan CL; Heo J; Sintchak MD; Schreiter E; Ludden PW Life on Carbon Monoxide: X-ray structure of Rhodospirillum Rubrum Ni-Fe-S Carbon Monoxide Dehydrogenase. Proc. Natl. Acad. Sci. U. S. A 2001, 98, 11973–11978. [PubMed: 11593006]

(43). Chen HJ; Wang Q; Lyu MQ; Zhang Z; Wang LZ Wavelength-switchable Photocurrent in a Hybrid TiO_2-Ag Nano- cluster Photoelectrode. Chem. Commun 2015, 51, 12072–12075.

(44). Attia YA; Buceta D; Blanco-Varela C; Mohamed MB; Barone G; Lopez-Quintela, M. A. Structure-Directing and High- Efficiency Photocatalytic Hydrogen Production by Ag Clusters. J. Am. Chem. Soc 2014, 136, 1182–1185. [PubMed: 24410146]

(45). Guo S-X; MacFarlane DR; Zhang J Bioinspired Electrocatalytic CO_2 Reduction by Bovine Serum Albumin-Capped Silver Nanoclusters Mediated by [α-$SiW_{12}O_{40}$]4−. ChemSusChem 2016, 9, 80–87. [PubMed: 26663883]

(46). Dobbek H; Svetlitchnyi V; Gremer L; Huber R; Meyer O Crystal Structure of a Carbon Monoxide Dehydrogenase Reveals a [Ni-4Fe-5S] Cluster. Science 2001, 293, 1281–1285. [PubMed: 11509720]

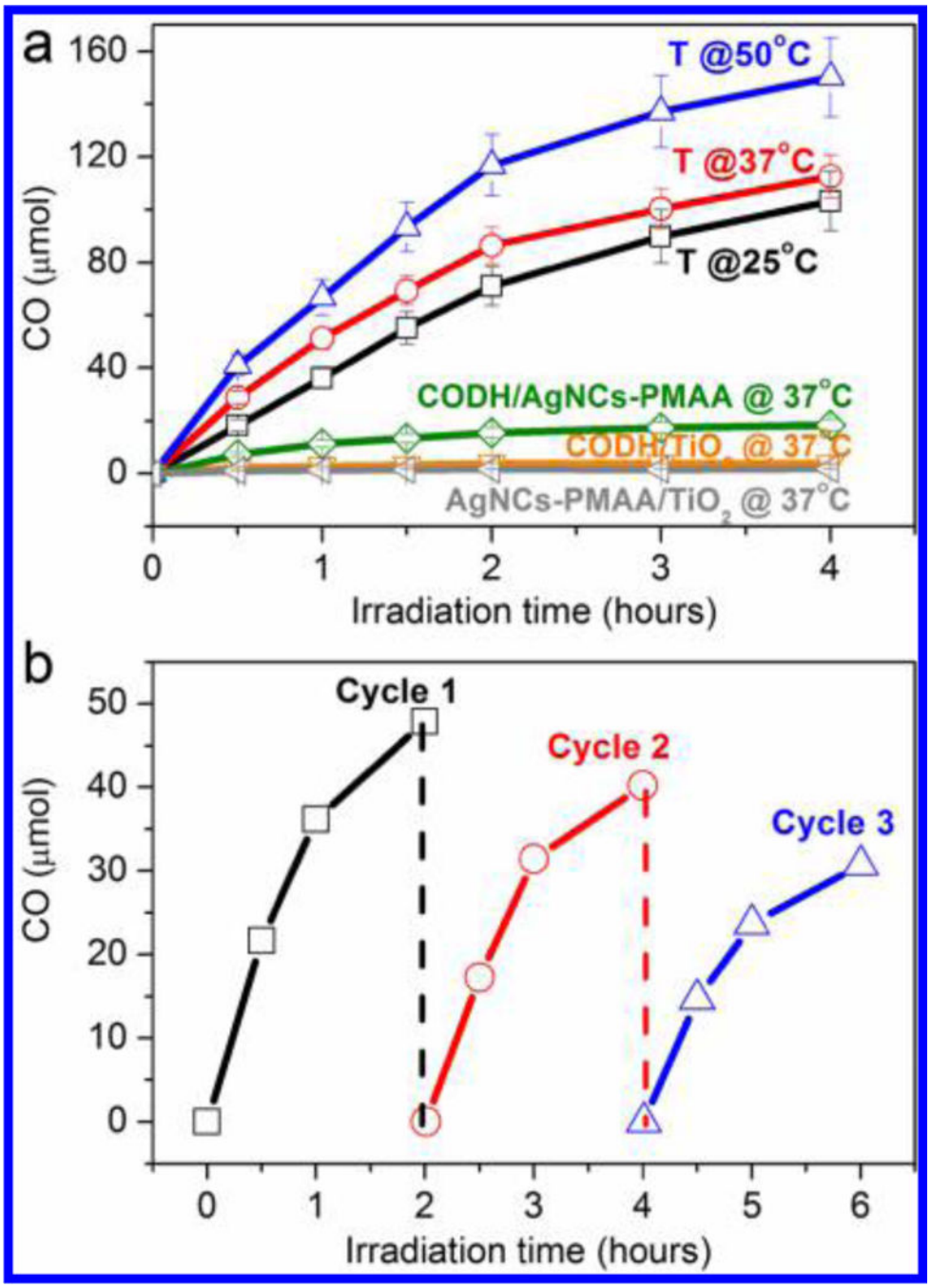

Figure 1.

Photocatalytic CO_2 reduction. (a) Time courses for photocatalytic CO production by the ternary CODH/AgNCs- PMAA/TiO_2 complex and other combinations, along with various control experiments, under visible light irradiation, followed using GC. In all cases, the 5 mL of water in the vial contained 0.1 M TEOA, 0.1 M NaCl, and 25 mM EDTA at pH 6.0. For experiments with the ternary complex (T), the vial contained 5 mg of AgNCs-PMAA/TiO_2 and 0.50 nmol of CODH. Experiments were carried out at 25 °C (black), 37 °C (red), and 50 °C (blue). Control experiments were carried out using CODH/AgNCs-PMAA

(no TiO_2), CODH/TiO_2 (no AgNCs-PMAA) and AgNCs-PMAA/TiO_2 (no CODH). (b) Production of CO over the course of 6 h, in which CO was flushed out at 2 h intervals and CO_2 was restored to the initial level (98%).

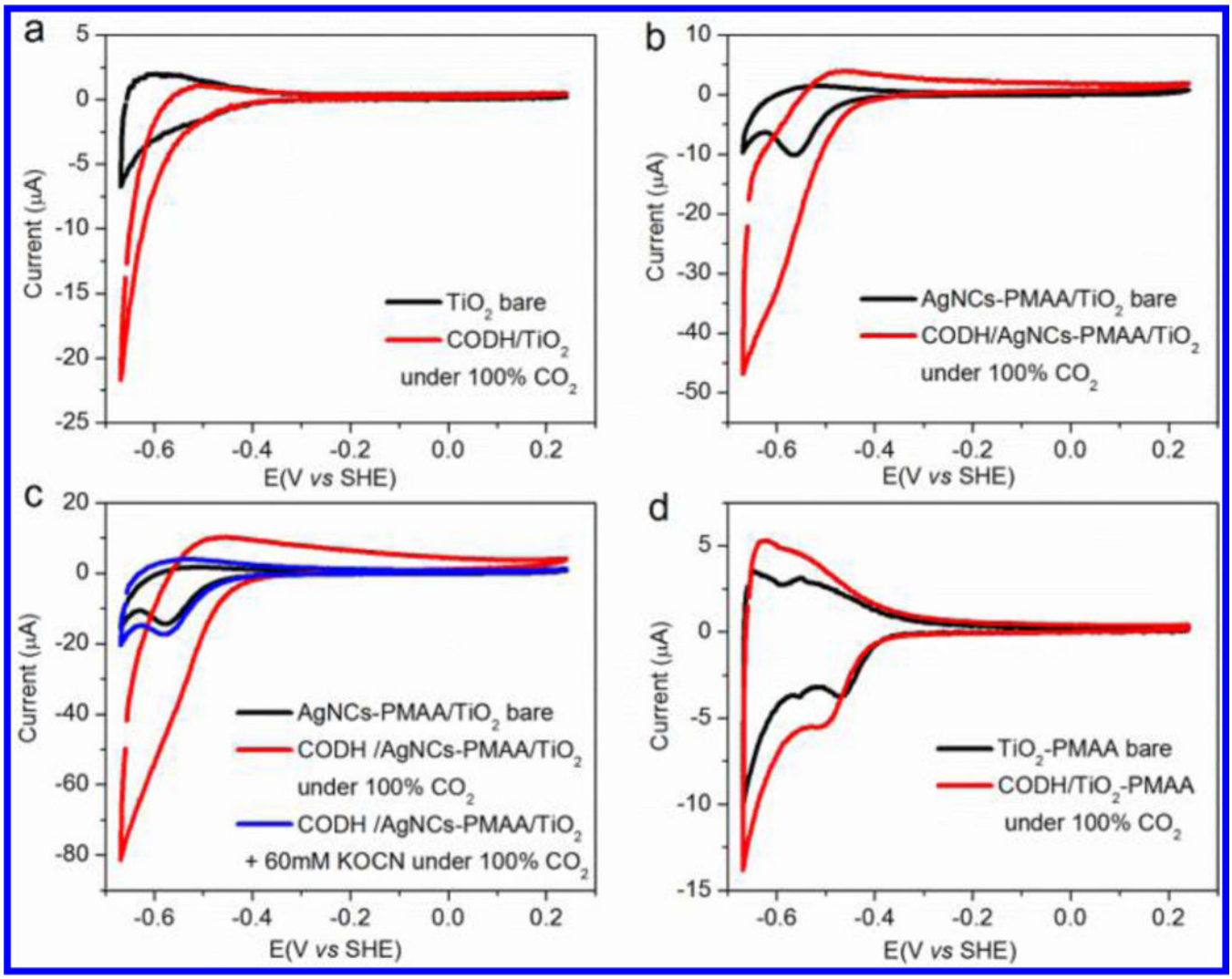

Figure 2.

Cyclic voltammograms of CODH adsorbed on variously modi fied TiO_2 electrodes under an atmosphere of 100% CO_2. (a) Electrocatalytic activity of CODH/TiO_2 and that of a bare TiO_2 electrode. (b) Electrocatalytic activities of CODH/AgNCs-PMAA/TiO_2 and AgNCs-PMAA/TiO_2 electrodes. (c) Selective inhibition of CO_2 reduction by CODH/AgNCs-PMAA/TiO_2 electrode in the presence of 60 mM KOCN. (d) E ffect of PMAA alone on electrocatalytic activity, observed by comparing CODH/PMAA/TiO_2 with PMAA/TiO_2. All solutions contained 0.2 M MES (pH 6.0, 0.1 M NaCl), with a temperature of 25 °C and a scan rate of 10 mV s^{-1}.

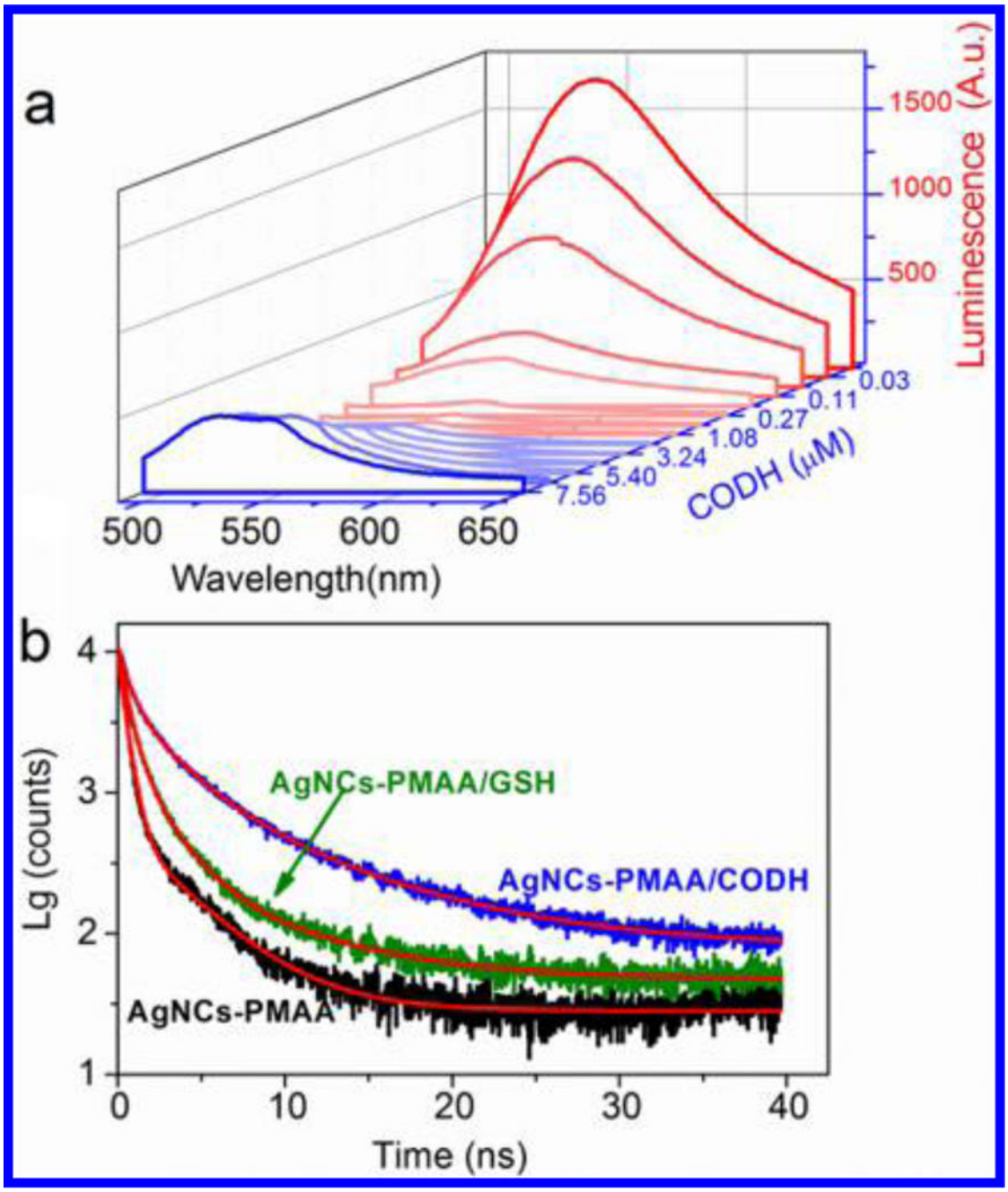

Figure 3.

Interaction between AgNCs-PMAA and CODH. (a) Photoluminescence spectra of AgNCs-PMAA (Ag atom concentration 20 μM determined by ICP-MS) using CODH (0−7.56 μM) in 0.2 M MES bu ffer (0.5 mL, pH 6.0) with λ_{ex} 460 nm. (b) Fluorescence decay traces of AgNCs-PMAA monitored at 460 nm. Black, green, and blue traces are for AgNCs-PMAA, AgNCs-PMAA/glutathione (GSH), and AgNCs-PMAA/CODH, respectively, in 0.2 M MES, pH 6, at room temperature. Fits are shown in red.

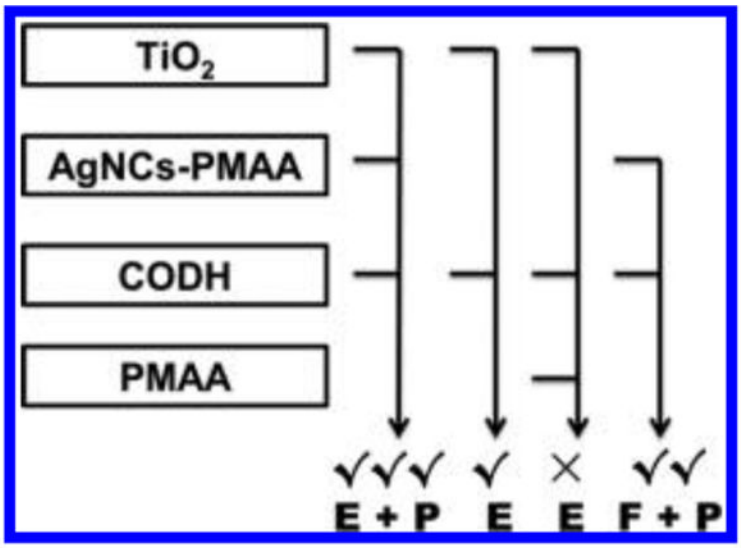

[a]The number of ticks (√) or no result (×) represent the performances and observations made for controlled-potential electrocatalysis (E), visible-light photoreduction (P), and fluorescence (F).

Scheme 1.
Connectivities between the Di fferent Components As Viewed in Various Experiments[a]

Table 1.

Visible-Light-Driven CO_2 Reduction by CODH/AgNCs-PMAA/TiO_2 Assemblies under Different Conditions

	CO[b] (μmol h^{-1})	TOF[c] (s^{-1})
standard condition[a]	36.12 ± 3.05	20 ± 2
Enzyme		
0.25 nmol	15.43 ± 2.52	17 ± 3
0.5 nmol	36.12 ± 3.05	20 ± 2
1 nmol	70.33 ± 5.55	19 ± 3
AgNCs-PMAA/TiO_2 Materials		
1 mg/mL	36.12 ± 3.05	20 ± 2
2 mg/mL	37.78 ± 4.10	21 ± 2
5 mg/mL	35.03 ± 2.22	19 ± 1
Temperature		
25 °C	36.12 ± 3.05	20 ± 2
37 °C	51.23 ± 2.32	28 ± 1
50 °C	66.75 ± 4.85	37 ± 3
pH		
6	36.12 ± 3.05	20 ± 2
7	33.72 ± 5.20	19 ± 3
Control Group		
AgNCs-PMAA/TiO_2	0.34 ± 0.20	N[d]
CODH/TiO_2	1.07 ± 0.52	0.06 ± 0.01
CODH/AgNCs-PMAA	11.36 ± 0.22	6 ± 0.3
Electron Donor		
TEOA	30.37 ± 2.58	17 ± 1
TEOA + EDTA	36.12 ± 3.05	20 ± 2
MES[e]	23.33 ± 2.22	13 ± 1

[a] Unless otherwise noted in the table, standard conditions were employed, which were as follows: CODH (50 μL of 10 μM solution) was added to a 5 mL dispersion of AgNCs-PMAA/TiO_2 (5 mg, composed of 3.05 mg of TiO_2 and 1.95 mg of AgNCs-PMAA, with Ag/Ti atom ratio of 0.27) in 0.1 M triethanolamine (TEOA), 25 mM ethylenediaminetetraacetic acid (EDTA), and 0.1 M NaCl at pH 6 and 25 °C. Irradiation was carried out with a Newport 67005 arc lamp (300 W) fitted with a 420 nm filter and located 5 cm from the solution.

[b] CO production rate (μmol of CO h^{-1}) based on the first hour of irradiation.

[c] Turnover frequency (TOF) expressed as molecules of CO produced per second per molecule of CODH).

[d] Value below 0.001 s−1.

[e] 2-(*N*-Morpholino)ethanesulfonic acid (MES).